Near-Field Electrospinning Patterning Polycaprolactone and Polycaprolactone/ Collagen Interconnected Fiber Membrane

Rox Middleton[1], Xia Li[2], Jenny Shepherd[3], Zhaoying Li[2], Wenyu Wang[2], Serena Best[3], Ruth Cameron[3], and Yan Yan Shery Huang[2]*

1. Department of Chemistry, University of Cambridge, Lensfield Rd, Cambridge CB2 1EW
2. Department of Engineering, University of Cambridge, Trumpington Street, Cambridge, CB2 1PZ, UK
3. Department of Materials Science and Metallurgy, University of Cambridge, 27 Charles Babbage Rd, Cambridge CB3 0FS
* Corresponding author: yysh2@cam.ac.uk

Solution based near-field electrospinning is employed to construct polymeric network membranes, made of orderly-arranged and interconnected fibres. The narrow tip-to-nozzle separation of the direct-writing process leads to solvent enriched fibres being deposited on the substrate, despite the use of a low boiling point solvent. This results in fibres with low cross-sectional aspect ratio (flattened appearance), but providing a unique opportunity to produce interconnected fibre junctions through *in situ*, localised solvent etching by subsequent fibre overlays. Orthogonal networks of polycaprolactone (PCL) fibres, or PCL/collagen composite fibres, are fabricated, and then characterised by microscopy and spectroscopy techniques. This study presents a direct approach to strengthen inter-fibre junctions, and further the feasibility to interweave and interconnect fibres of different properties, leading to networked membranes with potentially tailorable functions for tissue engineering applications and beyond.

Keywords: tissue engineering scaffolds; biofabrication; electrospinning; biodegradable polymer;

FIGURE FOR ToC_ABSTRACT
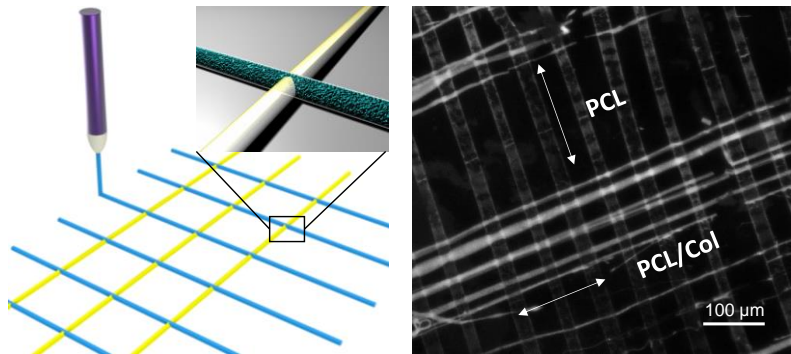
Orderly and interconnected fiber arrays are incorporated into thin membranes using near-field electrospinning. Orthogonal networks of polycaprolactone fiber membranes demonstrate superior mechanical properties arisen from the strong fiber junctions. Interconnecting polycaprolactone and polycaprolactone/collagen fibers is also demonstrated. This patterning approach may find uses in creating mechanically robust thin membrane, tailoring structural and functional properties for tissue engineering scaffolds and beyond.

1   Introduction

The ability to structure materials from the microscopic to the macroscopic scale is an important facet in harnessing diverse functionalities and applications of polymeric materials [1],[2],[3]. A number of methods have been investigated to form polymeric scaffolds from fibre structures, such as far-field electrospinning[4], centrifugal spinning[5], electro blow spinning[6] and pressurised gyration[7]. Despite their applications from filtration membranes to tissue engineering scaffolds[6],[8], the fibrous membranes produced by these methods are commonly limited by the ability to produce orderly patterns[9],[10],[11]. A further challenge associated with these existing techniques is the inability to create non-woven fabrics unless post deposition treatment is applied to obtain interconnected fibre junctions[12],[13],[14],[15]. Recent progress in precision electrospinning techniques, such as near-field electrospinning (NFES)[16],[17] electrohydrodynamic writing[18], and low-voltage electrospinning patterning (LEP)[19], has extended the fibre patterning capability, approaching that of a direct-writing fashion. Since these techniques rely on the close spineret-to-collector distance to obtain a stable jet, solvent evaporation may be incomplete depending on various parameters, including the target to collector distance[20]. For example, in the conditions where solvents are allowed to completely evaporate, a circular fibre cross-section is resulted[21],[22]. In contrast, when residual solvent is involved, surface properties of the collecting substrate will determine the fibre cross-sectional profile upon drying, and may further impart strong attachment between the fibres and the substrate[23],[24].

In this study, harnessing the potential of NFES in producing as-deposited solvent enriched fibres, we create biopolymer membranes of orthorgonal line patterns held by strong fibre interconnecting junctions which were formed *in situ* during the patterning process. By tuning the fibre-writing path, integrated membranes composing of polycaprolactone (PCL, a biodegradable polymer), or polycaprolactone/ collagen composite (PCL/col, with added collagen for potential bioactivity) fibres were demonstrated. Inter-changing the above two electrospinning solutions for patterning further allows us to connect and integrate PCL and PCL/col fibres into the same membrane structure. By improving the mechanical robustness of ultra-thin membranes, this capability may open up future uses in coupling and tailoring mechanical performance and biological functions for tissue engineering scaffolds.

2   Experimental Section

2.1   Solution preparation

To construct PCL fiber patterns, 1,1,1,3,3,3-Hexafluoro-2-propanol (HFP, from Sigma Aldrich) was used to dissolve 4 wt% to 8 wt% PCL (Mn=80,000 g/mol, Sigma Aldrich) to create the electrospinning solutions. Tetrahydrofuran (THF, Sigma Aldrich) was also tried as an alternative solvent, though less satisfactory patterns were formed (see Supporting Information, Figure S1).

For the PCL/col fiber patterns, a two-step solution preparation process was adapted. First, type I collagen from bovine Achilles tendon was immersed at 1wt% in HFP. After being swollen in HFP for 24 hours, the mixture was sonicated for 5 hours with a sonicator probe. The solution was viscous and of pale yellow color, with very few solids remaining. Any evaporated HFP during the sonication process was replaced in the same quantity. Subsequently, the 1wt% collagen-HFP solution was mixed with an 8wt% PCL-HFP solution at a 1:1 volume ratio. Hence, this yielded a 4.5wt% of PCL/col in HFP solution, where the PCL to collagen weight ratio is 8:1.

2.2   Near field electrospinning

Figure 1 (a) shows a schematic of the near-field electrospinning (NFES) setup and also the patterning procedure. The setup included a syringe pump (World Precision Instruments, AL-1000), a 1 ml syringe (BD Plastipak), a needle tip (BD Microlance, 19G), a high voltage power supply (Stanford Research Systems, INC., PS350/5000V-25W), an X-Y motion stage (PI micos, LMS-60; set at 100mm/s), and a Z motion stage (Thorlabs, L490MZ/M). The stage movement path was controlled by a Labview program written in house. The syringe needle was ground blunt and its outer diameter was 1.08 mm. The positive terminal of the high voltage power supply was attached to the syringe needle, and the collector was grounded. Silicon wafers (bare, or with a water soluble coating) were used as substrates for fiber deposition. The Z stage was adjusted so that the distance between the syringe tip and the substrate surface was ~1 mm. Some adjustments to the distance was required depending on the solutions, in order to avoid electrical arching. In a typical experiment, a voltage of 1000 V was applied between the spinneret and the deposition collector. The flow rate was adjusted to study its effects on pattern formation, as a result also to tune the fiber width. All fiber production was carried out at room temperatures of ~20°C, at humidity of 60-70%. A video showing the process of the NFES is included in the Supporting Information.

2.3   Tensile testing

For tensile testing, fibers were deposited onto silicon wafer substrates pre-coated with a water soluble coating (poly(4-styrenesulfonic acid), PSS) to allow membrane detachment. PSS solution (Mw ~75,000, 18 wt. % in water, Sigma Aldrich) was first diluted and thoroughly mixed with ethanol with a 1:5 weight ratio. A thin PSS coating on silicon wafer was formed by a spin-coater (Electronic Micro Systems Spin Coater Model 4000) with 100 rpm for 5 seconds, then 2000 rpm for 2 minutes. This PSS coated silicon wafer was then used as a substrate to collect the fibre membrane. To form robust thin membranes for substrate detachment, and mechanical testing, NFES with higher solution flow rates (~500 μL/min), which produces thicker fiber lines were adapted. To detach the thin membrane post deposition, the construct was merged into water for the dissolution of the PSS sacrificial layer. This process released the fibre membrane on to the water surface, which was then transferred to a manifold (see Supporting Information, Figure S2). Mechanical testing was carried out on a Hounsfield 5kN uniaxial extension instrument, at an extension speed of 1 mm/min. It is to note that samples need to be lifted and tested within 1 day of production, otherwise the bonding between the PSS sacrificial coating and the deposited membrane will be too strong to prevent the membrane release.

2.4   FTIR

Bruker FT-IR spectroscopy (reflection mode) was used to measure the solid samples. After collecting a background scan, the powder sample was placed in the spectroscopy. The absorbance was measured over $450 - 4000$ cm^{-1}. The spectrum was averaged over 50 scans. A new background scan was performed for each new sample.

2.5   Microscopy

To visualize the presence of the collagen, PCL/col composites were stained using a 0.1% w/v aqueous solution of Acriflavine (Fisher UK). Acriflavine shows affinity to collagen and has been previously applied in the imaging of collagen structures[25],[26]. To perform the characterization, samples were floated from the wafer and placed on a glass slide. A few drops of the staining solution were dropped onto the sample using a Pasteur pipette and left for 5 minutes. Careful rinsing was then carried out with deionized water. Imaging was carried out using a Leica SP2 confocal laser scanning microscope with excitation at 488 nm. For scanning electron microscopy (SEM) imaging of samples, a Philips XL30 sFEGSEM was used. Diameter measurements were performed on optical images, which were determined

manually using a line measurement tool in ImageJ. Histograms of the diameter distributions were shown in Supporting Information, Figure S3. It is noted that the diameter distributions do not exhibit a Gaussian profile, but an average and a standard deviation are reported for the fibre width nonetheless.

3   Results and Discussion

3.1   Patterning parameters

A number of processing parameters, including solvent choice, polymer concentration, and flow rates, were experimented to optimize fibre patterning during NFES. As shown in Figure 1 and in Figure S1 (Supporting Information), the use of HFP successfully produced uniform layered structures in parallel arrays, or orthogonal lattice. In contrast, THF was shown not to allow regular fibre formation, and produced beaded and broken fibres. Although both HFP and THF are hygroscopic solvents and are good solvents of PCL, HFP (boiling point of 59°C) was expected to undergo more rapid solvent evaporation than THF (boiling point of 66°C), depositing fibres with less residual solvents on the substrate. This may explain the fact that at similar flow rates, a higher polymer content needs to be dissolved in THF than HFP to minimise the spreading of the deposited line patterns. Moreover, beaded fibre morphology was observed in THF even at >10wt% polymer concentration. Other factors influencing fibre uniformity may be a result of the intrinsic solution properties such as solvent polarity, which should warrant additional systematic studies as a comparison to far-field electrospinning in the future.

For solutions containing pure PCL in HFP, uniform fibres were produced where the fibre line width was found to depend on the polymer concentration and the flow rate (when voltage and tip-to-substrate distance were kept constant). With a line speed of 100 mm/s, the writing of a single fibre layer on a 2 inch silicon wafer is in the order of minutes depending on the writing line density (see supporting video). A satisfactory patterning condition was found using 4 wt% PCL in HFP with varied flow rates to tune the fibre width. At a flow rate of ~200 µL/hr, a fibre width distribution of ~2 to ~20 µm (with mean 6.3±4.5 µm) was resulted; while at a high flow rate of ~2000 µL/hr, a fibre width distribution of ~90 to ~200 µm (with mean 135.9±40.5 µm) was resulted (see Figure 1(b)). Based on the above solution properties, composite fibres with PCL and collagen were further prepared (see Experimental Section). A solution combining 4 wt% PCL and 0.5 wt% collagen in HFP was used for final NFES. Such a mixed solution typically resulted in less regular fibre patterns (mean 7.5±4.8 µm) than the pure PCL counterpart. Thin fibres were also observed which underwent selected modes of bending instability, as shown in Figure 1(c).

3.2 Interconnected fibre junctions

Thin membranes were created with fibres patterned in layers of x-aligned and y-aligned fibres alternatively. For the current setup, since the exchange in fibre patterning between subsequent layers are done by rotating the silicon wafer by 90℃, the alignment between subsequent layers are not completely regular. It is expected that the fibre regularity can be further improved by incorporating an automatic process. Atomic force microscope (AFM) and scanning electron microscope (SEM) images of PCL grid patterns were shown in Figure 2 (a-c). These images show that the PCL fibres interfacing the substrate are flat bands with heights of below 0.5 μm, and with a cross-sectional aspect ratio of less than 1/10. Since fibres with almost complete solvent evaporation should exhibit an approximate circular fibre cross-section (with an aspect ratio of 1), the flat morphology of the PCL fibres strongly suggests that a significant amount of residual solvents are present post NFES deposition under our operating conditions. This is despite of the fact that HFP, a very low boiling solvent is used in comparison to other common solvents used for electrospinning PCL in the far-field regime[27]. Further evidence for the incomplete solvent evaporation was shown by the interconnected nature of the surface over the crossing horizontal and vertical fibres. Closer examination illustrates that crystalline patterns on the surface are extended over the joint (shown by both AFM and SEM). Finally, insignificant height difference was observed in the cross-sectional profile of multiple adjacent fibres.

3.3 PCL/collagen composite fibres

Figure 2(d) shows a typical SEM image of a composite membrane, which demonstrates similar network morphology as the pure PCL membrane, demonstrating interconnected junctions. There were however black spots, apparent pits in the fibres that had not been seen on the pure PCL sample. Fluorescence imaging and FTIR were used to characterise the presence of collagen in PCL/col composite membranes post NFES. FTIR in Figure S4 (Supporting Information) shows the presence of amide I and amide II peaks in the PCL/col composite membranes. The typical PCL absorption bands (carbonyl stretching at 1724 cm^{-1} and asymmetric C-O-C stretching at 1238 cm^{-1}) were observed in both pure PCL and PCL/col composite membranes. The positions of amide I and II peaks show slight shifts in PCL/col composite membrane comparing to the reference collagen I powder. The amide I peak shifts from 1627 cm^{-1} to 1653 cm^{-1} and the amide II peak shifts from 1526 cm^{-1} to 1545 cm^{-1}. Despite the slight change in peak positions, both amide I and II peaks are within the theoretical range (1800 − 1600 cm^{-1} for amide I and 1450 − 1550 cm^{-1} for amide II). These signals also compared well to previous far-

field electrospinning work[28]. Figure 2(e) illustrates spatial distribution of collagen contents by confocal microscopy for the PCL/col samples underwent acriflavine staining. Homogenous fluorescence was shown throughout the membrane structure, which suggests the absence of unmixed collagen clusters. To further prove that the fluorescence is specific to collagen, staining was performed on a membrane structure formed by orthogonally aligned fibres of pure PCL and PCL/col composites. Figure 2(f) indicates more pronounced fluorescence given rise by the PCL/col composite fibres than the PCL counterpart, confirming successful collagen inclusion post membrane release from the silicon water.

3.4   Mechanical properties of orthorgonally aligned, interconnected fibre membranes

The direct-writing attribute of NFES enables facile design of the fibre packing density (i.e. number of lines per unit width in the x-y directions) within the membrane. For mechanical testing, PCL membranes were constructed with 18 overlays (9 layers in each x and y directions), with each layer having a fibre density of 6 lines/mm. With a NFES condition leading to fibre widths of around 24 µm, this means that there are very few vertically overlapping fibres following shifted deposition (i.e. $9 \times 24 \times 6 = 1296$ µm *vs.* 1 mm). It was found that post-membrane release using the method shown in Figure 3(a), some fibres were broken during the process (example see Supporting Information). Nonetheless, membranes can be mounted in manifolds and characterised by tensile testing, where extension is applied in the direction along one of the fibre direction. Reproducible behaviours were observed for the PCL membranes produced under the same NFES parameters (see Figure S5, Supporting Information). Figure 3(b) grey curve, shows a typical plot of line force (force per unit width of membrane) versus sample strain. We observe seemingly three phases of mechanical deformation, with phase I being the elastic deformation, phase II the yielding process with maximum load achieved, and phase III the step-wise fibre breakage. During phase III, one could visualise fibres breaking sequentially from the outer edge inwards during the stretching process, supporting the mechanical data (highlighted by arrow labels in Figure 3(b)). Typical failure strains achieved under a 1 mm/min extension rate were between 400% and 600%, indicating strong interconnected junctions, and good fibre continuity.

With the prescribed network geometry, we can start to compare how the NFES membrane perform with respect to the theoretically expected membrane performance. This could act as an indicator to whether the patterning approach can potentially lead to designable membranes made to specifications. At a first approximation, one can assume that in the initial deformation stages (phase I and II), tensile loads are mostly bore by the aligned fibre direction. Taking an

average fibre dimension of 24 µm in width and 0.5 µm in height, and a cumulated fibre number of 54 lines per mm (6 lines/mm for 9 overlays in one NFES direction), the cumulated area per mm for the fabricated membrane is estimated to be 6.5×10^{-10} m^2/mm. With known Young's modulus (~300 MPa) and ultimate tensile stress (~14 MPa) of PCL of the same molecular weight[29], the NFES PCL membrane fabricated here would have an estimated stiffness of ~0.2 N/mm, and a maximum line force of ~0.01 N/mm. These values fall in the similar range as the experimental results (stiffness~0.06 N/mm, maximum line force~0.008 N/mm). The lower values of the experimental results can be explained by the fact that some fibres were damaged during the membrane release and transfer process; and the relaxed membrane structure would result in an apparent lower stiffness value. Nonetheless, results from the tensile experiments suggests that, designable and prescribed membrane properties can potentially be fabricated using the PCL-HFP solution system.

For the membranes formed by the PCL/col composite fibres, the samples proved to be significantly more fragile than the pure PCL samples. An example tensile behaviour of the PCL/col sample is shown in Figure 3(b) blue curve, as a comparison to the PCL sample. The poorer tensile performance could be a consequence of the pitted structure of PCL/col fibres, which further make them prone to breakage during the membrane release process. Another possible explanation could be that in our study, collagen crosslinking was not performed post fabrication. Hence, during the membrane release process, direct water contact may have weaken the structure of the PCL/col fibres which contains weakly water soluble collagen contents. Hence, the extent of fibre damage during the membrane release process is suggested to be the dominating factor controlling the mechanical performance. Depending on the applications, post-fabrication cross-linking of PCL/col fibres could be considered in the future to improve the mechanical properties. Nonetheless, as shown in the detailed view of the force-extension data in Figure 3(c), the mechanical behaviour of the membrane reflects those of the remaining intact fibres (shown by the camera images A-F). The fibre junctions interconnect orthogonally placed fibres, and can withstand substantial stretching (see images D & E). One can again observe stepwise decrease in the force level, which corresponds to distinct breakage of individually aligned fibres (see images D to F).

4 Conclusions and outlook

PCL and PCL/collagen fibres are successfully produced by NFES. Studying various parameters associated with the NFES process lead us to choose a 4 wt% polymer in HFP solution to create interconnected fibre networks. FTIR and confocal imaging of the PCL/collagen fibre samples

demonstrate the successful incorporation of collagen into the fibre structure; further, interconnected junctions are preserved in the composite fibre network. Tensile test showed that the PCL thin membrane exhibit good mechanical properties, which also underpins the potential of using NFES to structure interconnected fibre networks with tailored mechanical response. Although the biofunctionality of the PCL fibres can be potentially improved with the incorporation of collagen, our result show that the resulted mechanical property is significantly compromised. A potential avenue to overcome this would be to interweave and interconnect pure PCL and PCL/collagen fibres with appropriately designed overlays, or to impart collagen crosslinking post deposition. In summary, our study presents the feasibility to potentially mix and match desirable characteristics of different fibre types within thin network membranes for a wide range of applications.
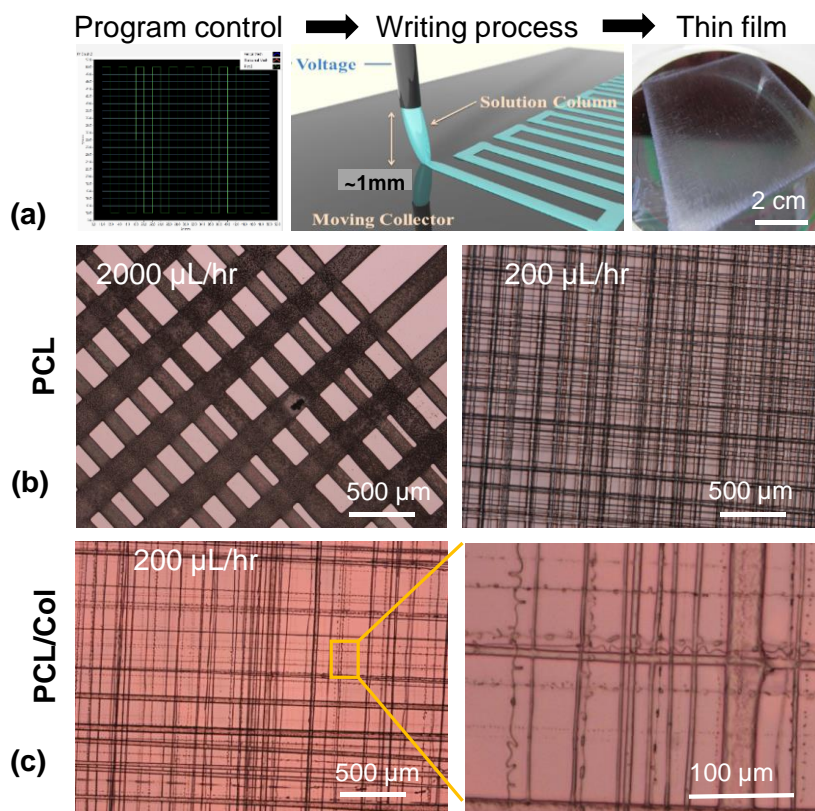
Figures

Figure 1. (a) Scheme of the NFES process for fabricating thin membrane structures. (b) PCL fibres produced with solutions of 4 wt% polymer in HFP, where varied widths can be tuned by solution flow rates. (c) PCL/col composite fibres produced with a combined 4 wt% PCL and 0.5 wt% collagen solution.
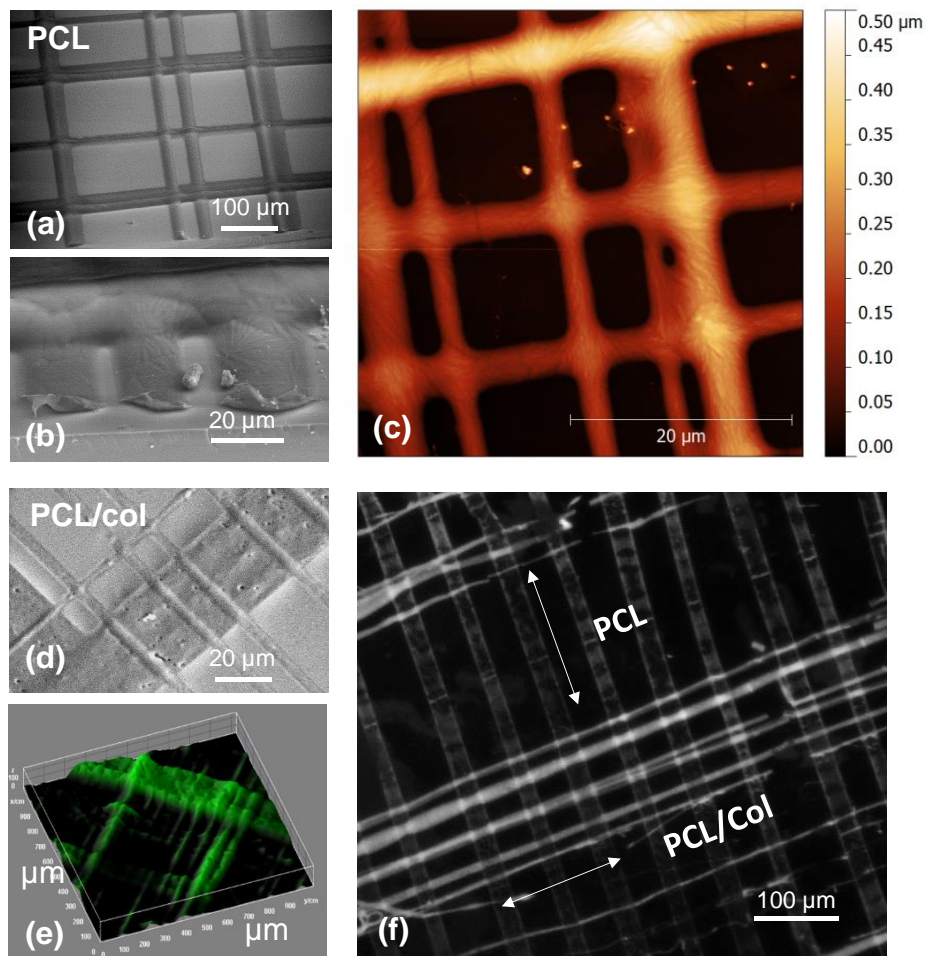
Figure 2. (a-c) Microstructures of PCL fibre network membrane imaged by SEM (a & b), and AFM (c). (d & e) Microstructures of PCL/col composite fibre network membrane imaged by SEM (d) and confocal microscopy (e), where the fluorescence is given rise by the acriflavine staining. (f) Confocal image of cross lattices of pure PCL fibres and composite PCL/col fibres.
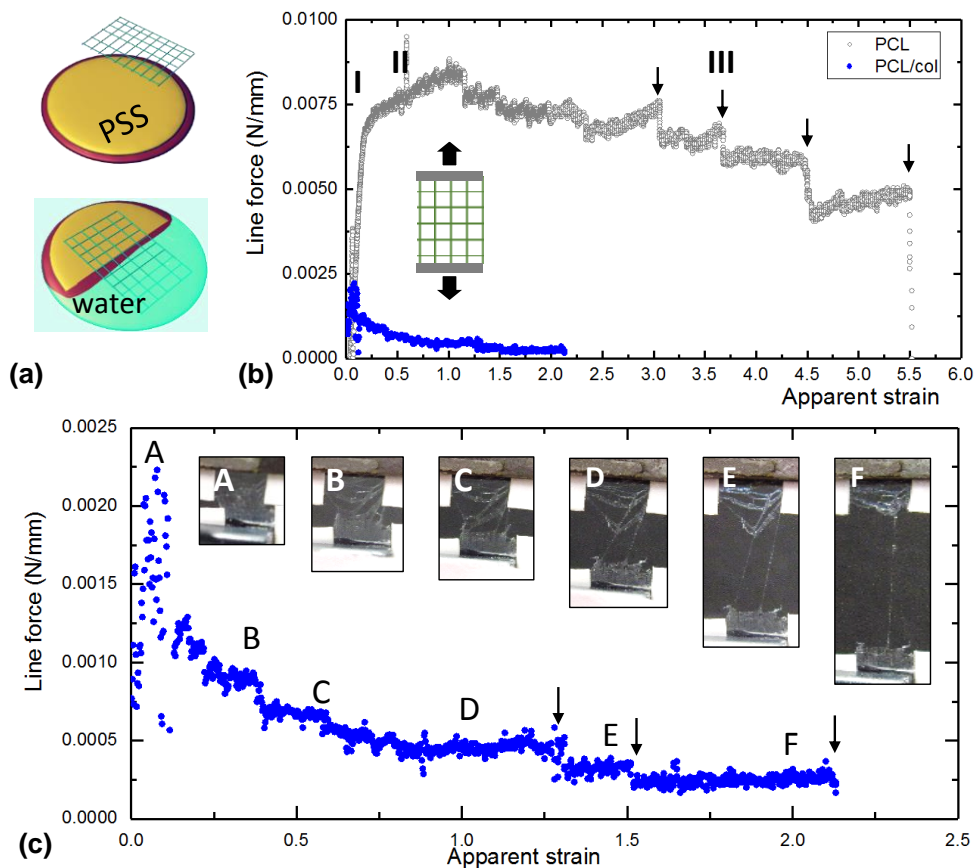
Figure 3. (a) Scheme of the membrane release process for producing samples for mechanical testing. (b) Line force versus apparent strain plots for a PCL fibre network (grey), where three deformation phases are identified, with arrows highlighting step-wise drop in force level in phase III. The deformation plot for a PCL/col network (blue) is also included as a comparison. (c) Zoom-in plot of the PCL/col composite network, with labels A-F which correspond the stages of deformation to the camera images (A-F).

Acknowledgements

5 Reference

[1] W. J. Li, C. T. Laurencin, E. J. Caterson, R. S. Tuan, F. K. Ko. *J Biomed Mater Res.* **2002**, *15*, 613-21.

[2] L. Moroni, J. R. de Wijn, C. A. van Blitterswijk. *Biomaterials*, **2006**, *27*, 974-85.

[3] P. X. Ma, Materials Today, **2004**, 7, 30-40

[4] J. Doshi. D. H. Reneker, *J. Electrostat*, **1995**, *35,* 151-160.

[5] X. Zhang, Y. Lu, *Polymer Reviews*, **2014**, *54*, 677-701

[6] Design and fabrication of flexible mesoporous Si-doped Al 2 O 3 ultrafine fibers by electro-blow spinning (EBS) technique. X Zhou, J Ju, Z Li, M Zhang, N Deng, B Cheng, W. M. Kang. *Ceramics International*, **2017**, *43*, 9729-9737

[7] S Mahalingam, M Edirisinghe. Macromolecular rapid communications 34, **2013**, 34, 1134-9

[8] Z. M. Huang, Y.-Z. Zhang, M. Kotaki, S. Ramakrishna, *Comp. Sci Tech.*, **2003**, *63*, 2223-2253.

[9] C. Y. Xu, R. Inai, M. Kotaki, S. Ramakrishna, *Biomaterials*, **2004**, *25*, 877.

[10] D. Li, Y. Wang, Y. Xia, *Adv. Mater.*, **2004**, *16*, 361.

[11] D. Zhang, J. Chang*, Nano Lett*, **2008**, *8*, 3283.

[12] S. J. Lee, S. H. Oh, J. Liu, S. Soker, A. Atala, J. J. Yoo. *Biomaterials*, **2008**, *29*, 1422-30.

[13] W. Wang, X. Jin, Y. Zhu, C. Zhu, J. Yang, H. Wang, T. Lin.*Carbohydr Polym*, **2016**, *140*, 356-61.

[14] H. Li, C. Zhu, J. Xue, Q. Ke, Y. Xia, *Macromol. Rapid Commun*, **2017**, *38*, 1600723.

[15] J Cheng, Y Jun, J Qin, SH Lee, *Biomaterials*, **2017**, *114*, 121-143

[16] D. Sun, C. Chang, S. Li, L. Lin, *Nano Lett*, **2006**, *6*, 839.

[17] C. Chang, K. Limkrailassiri, L. Lin, *Appl. Phys. Lett.*, **2008**, *93*, 123111.

[18] M. Rasekh, Z. Ahmad, R. Day, A. Wickam, M. Edirisinghe, *Adv. Eng. Mater*, **2011**, *13*, B296–B305

[19] X Li, Z Li, L Wang, G Ma, F Meng, RH Pritchard, EL Gill, Y Liu, YYS Huang, *ACS Appl. Mater. Interf.*, **2016**, *8*, 32120-32131.

[20] S. Y. Min, T. S. Kim, B. J. Kim, H. Cho, Y. Y. Noh, H. Yang, J. H. Cho, T.W. Lee, *Nat. Commun.*, **2013**, *4*, 1773

[21]Y. Lee, S. Y. Min, T. W. Lee. *Macromol. Mater. Eng.*, **2017**, 10.1002/mame.201600507

[22] Y. Lee, S. Y. Min, T. S. Kim, S. H. Jeong, J. Y. Won, H. Kim, W. Xu, J. K. Jeong, T. W. Lee. *Adv. Mater.*, **2016**, *28*, 9109

[23] Y. Y. S. Huang, E. M. Terentjev, T. Oppenheim, S. P. Lacour, M. E. Welland, *Nanotechn.*, **2012**, *23*, 105305.

[24] N. Xue, X Li, C Bertulli, Z Li, A Patharagulpong, A Sadok, YYS Huang, *PloS One*, **2014**, *9*, e93590

[25] M. Hanthamrongwit, R. Wilkinson, C. Osborne, W. H. Reid, M. H. Grant *J. Biomed Mat Res A*, **1994**, *28*, 213-216.

[26] M. McKegney, I. Taggart, M. H. Grant, *J. Mat Sci, Mat in Med*, **2001**, *12*, 833-844

[27] A. Cipitria,ab A. Skelton,a T. R. Dargaville,a P. D. Daltonac and D. W. Hutmacher, J. *Mater. Chem.*, **2011**, *21*, 9419-9453.

[28] N. Krithica, V. Natarajan, B. Madhan, P. K. Sehgal, A. B. Mandal, *Adv. Eng. Mater.,* **2012**, *14*, B149–B154

[29] S. Eshraghi, S. Das. *Acta. Biomater.*, **2010**, *6*, 2467-76.